

ROS-based Toolbox for Motor Parameter Identification of Robotic Manipulators

I. Ulici* A. Codrean* T. Natsakis*

* Automation department, Technical University of Cluj-Napoca,
Cluj-Napoca, Romania

Abstract: For many applications, a precise knowledge of the model of the robot is necessary for accurate and stable control. However, it is not always feasible or desirable to perform from scratch an in-depth study of the robot model, especially if it is not an element of concern for the respective application. In this article we present a methodology for identifying motor parameters of a robotic manipulator. We discuss the mathematical model and introduce an extensible toolbox with velocity-control based methodology for a fast identification of individual motor parameters. The results show that we can identify individual parameters even for joints that are commercialised as of the same type.

Keywords: identification for control, UR5 robot, ROS, robots manipulators

1. INTRODUCTION

Robotic manipulators are widely adopted in the automation of industrial production. They are able to perform in harsh conditions, or in repetitive, tedious work that would otherwise hinder resources and raise costs. Technical innovations allow expansive influence of robots in other territories, with service robotics, medical devices, agriculture, and logistics actively being developed [K.I.Goryanina et al., 2018]. Many of their use-cases require knowledge of the robot model, either to efficiently perform simulations before employing the real manipulator or for the development of model-based control.

Modelling of physical systems for control purposes is required to capture the main features of the system, while being mathematically tractable [Garulli et al., 2009]. To derive the model of a robotic manipulator we need the inertial parameters (such as mass and moments of inertia), and the parameters of the motors (friction, motor dynamics etc.). While mass parameters are often provided by the manufacturer, there is usually little to no information on the parameters of the motors of the robot. Assuming a rigid connection, these consist mainly of the torque-current characteristic of the motors and the friction coefficients between the elements of the joints.

The friction description depends on several characteristics: the geometry and roughness of contact surface, materials used, type of lubricant, velocity, humidity, temperature, wear, etc [Andersson et al., 2007]. Many friction models have been proposed in order to effectively define the friction dynamics, from the most common Coulomb model, to the addition of Stribeck function, to more complex state dependent models like Dahl, LuGre models [van Geffen, 2009].

A more detailed friction representation will add complex nonlinearities in the overall dynamic model. This could lead to a lengthier process in both the design and in the

actual runtime of the simulation, offering a higher model accuracy while taking away time that could be used for application architecture and experiments. Concurrently, any model-based controller would have a more convoluted configuration.

One of the defining characteristics of a motor is the torque-current coefficient. It is specific to the motor's design, including its magnetic strength, number of wire turns, armature length etc. The relation between current and torque is different, depending on whether the motor is a DC or an AC one, and can introduce several additional nonlinearities in the model.

The robot's full dynamic model incorporates the motor's aspects presented above. The motor can have other dynamics of its own, but a simplification may prove acceptable if the robot control is robust, be it the default implemented controllers of the robot itself or a newly designed one.

The kinetic and behavioural aspects of a robotic manipulator are expressed in the dynamic model, which relates joint torques to the robot motion. This model can vary in complexity, depending on the purpose it is used for. Identification of the dynamic parameters of the model can be approached from multiple angles [Madsen et al., 2020]:

- Disassembly of each link and joint in order to directly evaluate mass, moments of inertia, joint friction etc. However this process is a tedious one, with time consumed for the manual operations, and it needs reiteration if any hardware changes occur.
- Computer Aided Design (CAD) allows the dynamic parameters of each link to be found using nominal geometric and material characteristics. Nonetheless, the CAD parts may not be identical to the physical correspondents and thus the accuracy of the parameters is decreased. Furthermore, the motor parameters are not available.

- System identification strategies, which analyse the input-output behaviour of the robot, are preferred due to their flexibility, reliability, and availability.

Various models are implemented in literature, using the Lagrangian, Newton-Euler or Kane formulations as a starting point [Sciavicco et al., 1995, Jubien et al., 2014, Ni et al., 2019, Madsen, 2020]. From that, several other additions may be introduced, for a more accurate model: taking into consideration the flexibility of the joints [Madsen et al., 2020, Madsen, 2020, Zollo et al., 2014], selecting an appropriate friction model [Khan et al., 2016, Madsen, 2020], adding action of external forces, modelling disturbances, favoring the nonlinear motor torque coefficient over an approximation and other similar decisions.

This article presents the methodology used for a fast and accessible identification of torque-current and friction coefficients in a set of motors. We derived a simplified dynamic model that can be generalised to other types of robotic manipulators, and implemented an identification toolbox that can be used out-of-the-box. For the purpose of demonstrating and assessing the identification of motor parameters under simplification hypotheses, we conducted experiments on a UR5 (Universal Robots, Odense, Denmark). The UR5 robotic arm belongs to a family of collaborative robots with great flexibility, designed specifically for safe operation near humans. This specific robotic manipulator accommodates integrated strain wave gearboxes, brushless AC permanent magnet synchronous motors (PMSM), position sensors, and brakes.

The article is structured as following: Section 2 expands on the mathematical equations of the UR5, discussing some modelling variations, while section 3 explains the methodology reasoning and implementation of the identification process. The experiments' results are provided in section 4. Finally, section 5 discusses the implications and validity of the experiments and the accessibility of the method compared to other approaches.

2. MATHEMATICAL MODEL

The UR5 robot is a six degree of freedom robot with six revolute joints, each with a range of $(-2\pi, 2\pi)$ with velocities up to π rad/s. Fig. 1 displays the physical depiction of the robot.

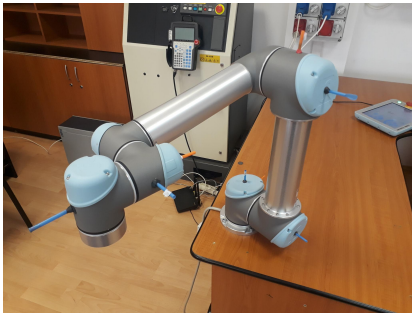


Fig. 1. The UR5 robot. The blue straws represent the positive direction of the axes of rotation of the joints.

The joint coordinates are defined as q , where $q = [q_1, q_2, q_3, q_4, q_5, q_6]^T$, and q_i represents the angle value cor-

responding to the i -th joint. Likewise, the joints velocities, accelerations and torques are defined as vectors \dot{q}, \ddot{q}, τ .

The forward kinematics allow computation of the pose of a robot's end-effector, given the state of the joints. The UR5 kinematic model is constructed using the standard Denavit-Hartenberg parameters [Denavit and Hartenberg, 1955, 1965] already provided by the manufacturer, summarized in table 1. Using this convention, each link has four parameters assigned to it, depending on its own and subsequent frames of coordinates: link length r , link rotation angle α , joint angle θ and link offset d .

Table 1. D-H parameters for the UR5

Link	θ_i [rad]	d_i [m]	r_i [m]	α_i [rad]
1	q_1	0.1519	0	$\pi/2$
2	q_2	0	-0.425	0
3	q_3	0	-0.39225	0
4	q_4	0.10915	0	$\pi/2$
5	q_5	0.09465	0	$-\pi/2$
6	q_6	0.0823	0	0

Table 2. Mass properties of the UR5

Link	Mass[kg]	Center of Mass Position[m]
1	3.7	[0, -0.02561, 0.00193]
2	8.393	[0.2125, 0, 0.11336]
3	2.33	[0.15, 0, 0.0265]
4	1.219	[0, -0.0018, 0.01634]
5	1.219	[0, 0.0018, 0.01634]
6	0.1879	[0, 0, -0.001159]

The dynamic model takes into consideration the forces and torques acting on the robot, as well as the kinetic properties of the manipulator (mass, moments of inertia, center of masses, joint elasticity, friction, etc). The mass properties of the UR5 are collected in table 2, as declared by the manufacturer. Each of the robots in the UR series have these parameters available. Moreover, the user of the identification toolbox has the freedom to edit them corresponding to their own robot.

In order to discuss the dynamic modelling and its simplification, we formulate a general system of equations as such:

$$M(q)\ddot{q} + C(q, \dot{q})\dot{q} + G(q) = \tau_m - \tau_{ext} - \tau_{dist} - \tau_f \quad (1)$$

where M is the inertia matrix, C the matrix of centrifugal and Coriolis forces, G the vector of gravitational torque or force. The right side of the equation is composed of the motor torque τ_m , external torques τ_{ext} , a disturbance term τ_{dist} and the friction torques τ_f that act on the joint.

The dynamics involved in the joints are portrayed in (1) and depend on position, velocity, and acceleration. The experiment has been thought to not have any external forces acting on the robot, in order to simplify the workflow. The disturbances will not be modelled, based on the assumption that the experiment's movements are simple and isolated, and that the identification process will issue generally valid parameters.

In the case of DC motors, the torque-current characteristic is proportional:

$$\tau_m = k_{ct}i \quad (2)$$

where i represents the currents sent to the motors.

That is not the case with AC motors, where the torque current characteristic is nonlinear and difficult to model [Rusnicki et al., 2015, Restrepo and Gautier, 1995]. However, Restrepo and Gautier [1995] showed that k_{ct} can be approximated with two methods: taking mean or median value of the ratio E_m/q_m - where E_m and q_m are the amplitude of sinusoidal emf (DC electromotive force voltage) between 2 phases, respectively the rotor velocity; or using an equivalent DC motor methodology to represent the AC configuration. Both cases allow the treatment of k_{ct} as a constant. In order to have variables that are easy to measure and as few as possible in the robotic model, the function of the motor torque will therefore be a linear one as in (2).

Joint friction is another nonlinearity that has been discussed in literature and proved to have an acceptable simplification for robotics application consisting of only the Coulomb and viscous friction [F.Marques et al., 2016], that is

$$\tau_f = k_{fc}sign(\dot{q}) + k_{fv}\dot{q}, \quad (3)$$

where the $sign$ function is defined as

$$sign(x) = \begin{cases} +1, & x > 0 \\ -1, & x < 0 \end{cases} \quad (4)$$

Putting together (1), (2), (3), and taking into consideration aforementioned simplifications, the general relation used to describe the dynamics becomes:

$$k_{ct}i = k_{fc}sign(\dot{q}) + k_{fv}\dot{q} + M(q)\ddot{q} + C(q, \dot{q})\dot{q} + G(q) \quad (5)$$

The identification process will use this robot model for the parameter analysis.

3. PARAMETER IDENTIFICATION EXPERIMENT AND METHODOLOGY

3.1 Model used for the identification

Parameter identification has been generally approached by computing a set of base parameters as a linear combination of dynamic coefficients, employing search algorithms from least square method [Atkenson et al., 1986] to genetic algorithms, artificial bee colony algorithms [Ding et al., 2015], weighted maximum likelihood estimation [J.Swevers et al., 2007] and other methods that use a regressor matrix. These methods would demand experiments with a specific optimised trajectory [Swevers et al., 1997] that also has to be calculated according to the base parameters.

To reduce the time consumed on experiments and the identification process, the identification algorithm searches just for the torque-current (k_{ct}) and friction (k_{fc} , k_{fv}) coefficients, considering the other parameters (mass, inertia) known from the manufacturer specifications. Furthermore, the experiments will consist of trajectories of constant velocities, thus eliminating a degree of variability with the joint acceleration term. This feature changes (5) into:

$$k_{ct}i = k_{fc}sign(\dot{q}) + k_{fv}\dot{q} + C(q, \dot{q})\dot{q} + G(q) \quad (6)$$

The gravity term G is computed automatically depending on the state and mass properties of the robot, using the Recursive Newton Euler Algorithm [J.Y.S.Luh et al., 1980] without taking acceleration terms into account. The centrifugal matrix C is derived from the Euler-Lagrange formulation of the dynamic model [Spong and Vidyasagar, 2006]. G and $C\dot{q}$ are computed with regards to all the joints' measured position and velocity, ending up being column vectors. However, since each motor undergoes the identification procedure separately, only the element corresponding to that joint will be taken into consideration.

We performed measurements of current, position, and velocity for each joint independently to identify and analyse the torque-current (k_{ct}) and friction (k_{fc} , k_{fv}) parameters, based on (6). This takes into account the individuality of each of the joints' parameters, but can also serve as a valid comparison between different joints of the same type. The procedure allows for fewer cross-correlated joint disturbances in the measurements. Fig. 2 depicts a sample measurement.

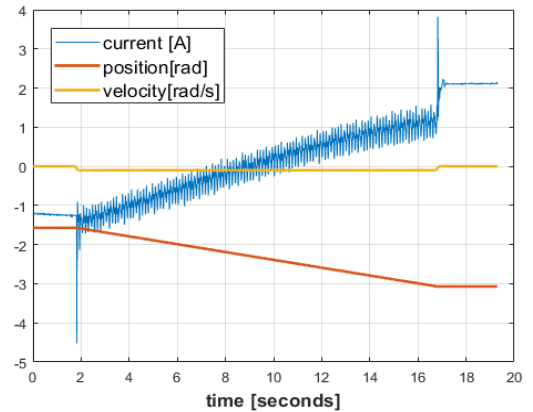


Fig. 2. Sample measurement of a joint moving under constant velocity. The position (red), velocity (yellow), and current (blue) are visible for the duration of the measurement

Considering a movement of constant \dot{q} , (6) can be written in terms of the measured current for each joint:

$$i_j = \frac{k_{fcj}sign(\dot{q}_j) + k_{fvj}\dot{q}_j + G_j(q) + C_{j,j}(q, \dot{q})\dot{q}_j}{k_{ctj}} \quad (7)$$

with $j = \{1, \dots, 6\}$. Current i_j , positions q , and velocities \dot{q} are all varying with time.

3.2 Experiment preparations

Some details need attention in order for the identification algorithm to properly work. The mounting of the robot influences the gravity forces that act on it. In our case the robot was mounted with the axis of rotation of the first joint parallel to the gravitational field, the gravity term for that joint was therefore zero. This makes (6) redundant, and we cannot identify k_{ct} , k_{fv} and k_{fc} at the same time. We choose therefore to use a predefined value for the torque-current coefficient (e.g. approximated from the other two joints of the same type), so the search would be run only for the friction coefficients.

To avoid having a zero gravity term for the last joint as well, we attached a mass off the axis of rotation of joint 6. To have more uniform and accurate results, we attached the same mass to the robot while performing the identification on the smaller joints (4th, 5th and 6th). A photo of the added mass can be seen in Fig. 3.



Fig. 3. Added mass off the axis of rotation, used for the identification of joint 4, 5, and 6

3.3 Identification procedure

For each joint, the parameter identification consists of three stages:

- (1) The identification of torque-current coefficient k_{ct} and the total friction torque τ_f
- (2) The identification of viscous k_{fv} and Coulomb friction parameters k_{fc}
- (3) The analysis of all acquired data to find a triple (k_{ct}, k_{fv}, k_{fc}) as the conclusive parameters for each joint.

For a single joint, the data from one experiment can be written in the next matrixial form:

$$\begin{bmatrix} i_{m1} \\ i_{m2} \\ \vdots \\ i_{mn} \end{bmatrix} = \begin{bmatrix} \text{sign}(\dot{q}_m) & \dot{q}_m & G(q_1) + C(q_1, \dot{q}_m)\dot{q}_m \\ \text{sign}(\dot{q}_m) & \dot{q}_m & G(q_2) + C(q_2, \dot{q}_m)\dot{q}_m \\ \vdots & \vdots & \vdots \\ \text{sign}(\dot{q}_m) & \dot{q}_m & G(q_n) + C(q_n, \dot{q}_m)\dot{q}_m \end{bmatrix} \cdot \begin{bmatrix} k_{fc}/k_{ct} \\ k_{fv}/k_{ct} \\ 1/k_{ct} \end{bmatrix} \quad (8)$$

i_{mn} , q_n correspond to the n^{th} timestep from measurement m , while q_m is the velocity used for the respective measurement.

The system does not have a solution because the matrix from (8) does not have full rank. This comes as a consequence of the first two columns that are linearly dependent, having the same values all through, since velocity q_m is fixed.

To overcome this, we combine the friction terms into $\tau_f = k_{fc} \cdot \text{sign}(\dot{q}_m) + k_{fv}\dot{q}_m$, obtaining:

$$i_{mn} = \tau_f + \frac{G_{mn} + C_{mn}\dot{q}_m}{k_{ct}} \quad (9)$$

for which a solution can be found.

The first stage (identification of k_{ct} and τ_f) is executed on iterations of the same velocity, using the Nelder-Mead minimization [Nelder and Mead, 1965] for the fitting of the current.

The second stage (identification of k_{fv} and k_{fc}) takes the pairs of \dot{q} and τ_f from all measurements of different velocities and uses (8) for a new fitting.

Fig. 4 presents the fitting results respective to the measurement from Fig. 2 as a comparison between the measured and estimated current, with parameters $k_{ct} = 12.0167$ and $\tau_f = -7.3853$.

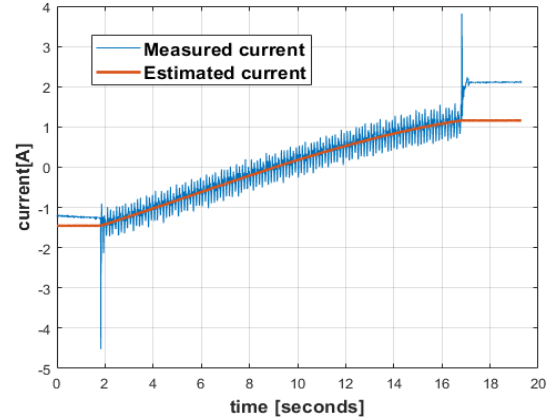


Fig. 4. Sample of current fitting

3.4 Software implementation aspects

The software package that aids in the identification process is making use of both the Robot Operating System (ROS) utilities [Stanford Artificial Intelligence Laboratory et al., 2018] and an analysis tool of preference between [MATLAB, 2020] and Python [Rossum and F.L.Drake, 2009].

ROS is an open-source framework designed for robot software applications. The robotic arms from the Universal Robots company benefit from community support and an already implemented ROS driver. While connected to ROS, the UR5 can perform different pre-defined tasks, coded specifically for the identification workflow, and provide enough real-time data to be later investigated and interpreted.

We used two controllers from the *Universal robots ROS driver*, provided by Universal Robots: a *trajectory position controller*, that is used to position the robot in the initial state before a measurement, and the *joint group velocity controller* that is used to perform the motions for the identification process. Initial joint positions, distance of travel, velocities, and number of iterations are all read from an input file that the user fills in with desired values prior to a round of experiments.

For the identification process, the user may choose between the provided MATLAB and Python applications, depending on their own setup and experience. It can easily be conducted using the provided application and its documentation, found at [https://gitlab.utcluj.ro/true-rehab/robot-identification]. The measurements are employed from ROS and are automatically collected in bag files once the experiment starts. The user then has to import those files in

the identification toolbox and select the type of robot he is working with, after which the identification process is commenced.

4. RESULTS

The first identification stage from the experiments delivered results concerning the torque-current constant k_{ct} . Fig. 5 and 6 present the characteristic of the torque-current relationship with respect to velocity, grouped by type of motor. By reasons of safety, the second and third joint were analysed in the $(-1,1)[\text{rad/s}]$ range.

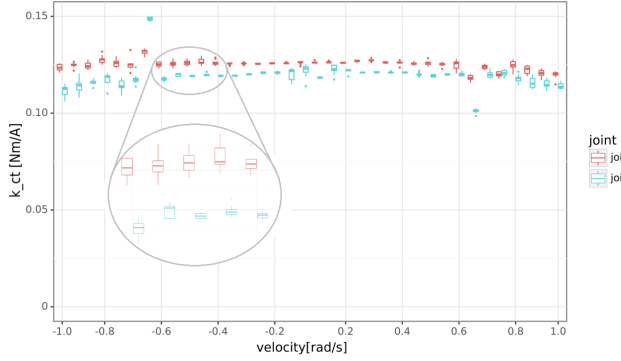


Fig. 5. Joint 2, joint 3 torque-current coefficient comparison. Each box expands between the 1st and 3rd quartile of the torque-current coefficient for a specific velocity. An additional line is positioned at the median. The whiskers show the data below and above the 1st and 3rd quartile respectively.

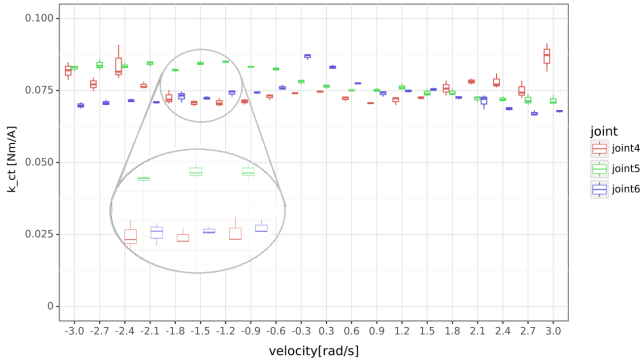


Fig. 6. Boxplots summarising the torque-current coefficients for joint 4, joint 5, and joint 6

The friction coefficients, k_{fv} and k_{fc} have been found by first taking the means of the torque-current coefficient for each velocity and then using those values in a second fitting stage. A batch of measurements for the friction identification consists of one measurement for each velocity in the chosen range. Fig. 7 and 8 show the distribution of the friction coefficients. For each joint an average is made to use in the model.

The resulting coefficients are presented in table 3. The k_{fc} and k_{fv} values are uniquely determined for each joint in the second stage, while the k_{ct} final value is obtained by averaging the coefficients found for all the velocities.

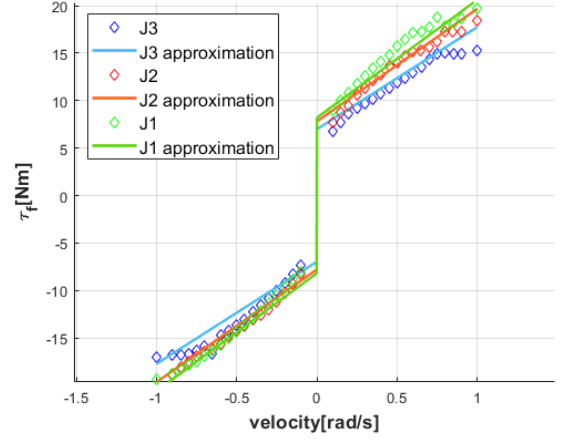


Fig. 7. Friction term comparison for joint 1, 2 and 3. While the dotted points represent the calculated full friction term τ_f from the first step of the identification with regards to velocity, the lines are drawn using (3) with the k_{fv} and k_{fc} that were identified.

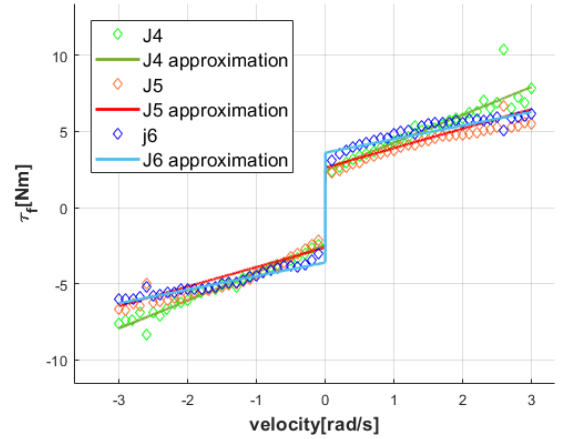


Fig. 8. Friction term comparison for joint 4, 5 and 6

Table 3. Final results for the torque-current, viscous and Coulomb coefficients

Joint	k_{ct}	k_{fv}	k_{fc}
1	12.3	8.1272	12.3141
2	12.6351	7.7891	11.881
3	12.0383	6.9762	10.7667
4	7.7366	2.4405	1.8286
5	7.9228	2.6265	1.2794
6	7.4723	3.6058	0.8921

5. DISCUSSION

Fig. 5 and 6 show that for each velocity used in the experiments, the torque-current values resulting from different measurements exhibit low variability for each joint. However joints of the same type present a difference in the mean of the coefficient, which may further affect the identification of friction coefficients and ultimately the parity between the model and the real robot. The final values of k_{ct} , k_{fv} and k_{fc} indicate the particularity of each joint, even if the first three and the last three adhere to the same type of motor. This highlights further the need for

a joint-by-joint identification both for the torque-current and friction coefficients.

The friction model we used in the identification adopted only the viscous and Coulomb friction terms expressed in relation (3), without other nonlinear characteristics. This implies the existence of a slope proportional to the joint velocity and an offset conditioned by the sign of the same velocity. However, the system is in fact a flexible joint manipulator robot, with the joint torques and friction depending on both the link and rotor angular positions. Furthermore, more complete friction models of robot joints have been described in literature [Andersson et al., 2007], [F.Marques et al., 2016]. Nevertheless, our results indicate that the simple friction formulation can capture most of the system's behaviour. The additional accuracy that would come from modelling the joints as flexible ones would also imply the cost of twice the number of generalized coordinates [Madsen, 2020], hence a more complicated identification process. Furthermore, the direct assessment of rotor positions may not be available or would require heavy preparation.

Determination of joint-specific motor parameters may increase accuracy in simulations and behaviour analysis of the system, but it could also help in model-based control design for specific manipulator robots. The simple and precise model that results from our proposed identification methodology can cut back on time and resources in first stages of robot application implementation, allowing users to focus on the target application.

ACKNOWLEDGMENT

This work was supported by a grant of the Romanian Ministry of Education and Research, CNCS - UEFISCDI, project number PN-III-P1-1.1-TE-2019-1975, within PNCDI III.

REFERENCES

- Andersson, S., Söderberg, A., and Björklund, S. (2007). Friction models for sliding dry, boundary and mixed lubricated contacts. *Tribology International*.
- Atkenson, C., C.H.An, and J.M.Hollerbach (1986). Estimation of inertial parameters of manipulator loads and links. *The International Journal of Robotics research*.
- Denavit, J. and Hartenberg, R. (1955). A kinematic notation for lower-pair mechanisms based on matrices. *Trans ASME J. Appl. Mech* 23: 215–221.
- Denavit, J. and Hartenberg, R. (1965). Kinematic synthesis of linkages. *McGraw-Hill series in mechanical engineering. New York: McGraw-Hill. pp. 435*.
- Ding, L., Wu, H., Yao, Y., and Yang, Y. (2015). Dynamic model identification for 6-dof industrial robots. *Journal of Robotics*.
- F.Marques, J.C., P.F., Claro, P., and Lankarani, H. (2016). A survey and comparison of several friction force models for dynamic analysis of multibody mechanical systems. *Nonlinear Dynamics* 86 1407-1443.
- Garulli, A., Tesi, A., and Vicino, A. (2009). Uncertainty models for robustness analysis. *Control Systems, Robotics, And Automation vol IX*.
- J.Swevers, W.Verdnock, and Schutter, J.D. (2007). Dynamic model identification for industrial robots. *IEEE Control Systems*.
- Jubien, A., Gautier, M., and Janot, A. (2014). Dynamic identification of the kuka lwr robot using motor torques and joint torque sensors data. *IFAC Proceedings Volumes, 47(3)*.
- J.Y.S.Luh, M.S.Walker, and R.P.C.Paul (1980). On-line computation scheme for mechanical manipulators. *Journal of Dynamic Systems Measurement and Control*.
- Khan, Z.A., Chacko, V., and Nazir, H. (2016). A review of friction models in interacting joints for durability design". *Advances in Mechanical Engineering*.
- K.I.Goryanina, A.D.Lukyanov, and O.I.Katin (2018). Review of robotic manipulators and identification of the main problems. *XIV International Scientific-Technical Conference Dynamic of Technical Systems*.
- Madsen, E. (2020). *Joint dynamics and adaptive feed-forward control of lightweight industrial robots*. Ph.D. thesis, Aarhus University.
- Madsen, E., Aagaard, S., Norbert, T., Ujfalusi, A., Rosenlund, O.S., Brandt, D., and Zhang, X. (2020). Dynamics parametrization and calibration of flexible-joint collaborative industrial robot manipulators. *Mathematical Problems in Engineering*.
- MATLAB (2020). *version 9.8.0.1359463 (R2020a)*. The MathWorks Inc., Natick, Massachusetts.
- Nelder, J. and Mead, R. (1965). A simplex method for function minimization. *The Computer Journal*, 7.
- Ni, H., Zhang, C., Hu, T., Wang, T., Chen, Q., and Chen, C. (2019). A dynamic parameter identification method of industrial robots considering joint elasticity. *International Journal of Advanced Robotic System*.
- Restrepo, P. and Gautier, M. (1995). Calibration of drive chain of robot joints. *International Conference on Control Applications*.
- Rossum, G. and F.L.Drake (2009). *Python 3 Reference Manual*. CreateSpace, Scotts Valley, CA.
- Rusnicki, T., R.Czerwinski, Polok, D., and Sikora, A. (2015). Performance analysis of a pmsm drive with torque and speed control. *Mixed Design of Integrated Circuits and Systems*.
- Sciavicco, L., Siciliano, B., and V.Luigi (1995). Lagrange and newton-euler dynamic modeling of a gear-driven robot manipulator with inclusion of motor inertia effects. *Advanced Robotics*, 10, 317–334.
- Spong, M.W. and Vidyasagar, M. (2006). *Robot dynamics and control*. John Wiley and Sons.
- Stanford Artificial Intelligence Laboratory et al. (2018). Robotic operating system. URL <https://www.ros.org>.
- Swevers, J., Ganseman, C., Tukel, D., de Schutter, J.V., and Brussel, H. (1997). Optimal robot excitation and identification. *Transactions on Robotics and Automation Robotics*, 13.
- van Geffen, V. (2009). A study of friction models and friction compensation. *Materials Science*.
- Zollo, L., Lopez, E., Spedaliere, L., Garcia, N., and Guglielmelli, A.E. (2014). Identification of dynamic parameters for robots with elastic joints. *Advances in Mechanical Engineering*.